MOLEKUL
eISSN: 2503-0310

Articles
https://doi.org/10.20884/1.jm.2023.18.1.8123

Photodegradation and Photoelectrodegradation of Methyl Orange and Methyl Violet Dyes using Graphite/$PbTiO_3$ Composite under Visible Light Irradiation

Candra Purnawan[1,2]*, Sayekti Wahyuningsih[2], Erick Ryan Yulianto[2], Ozi Adi Saputra[2]

[1]Analytical and Environmental Chemistry Research Group, Universitas Sebelas Maret,
Surakarta 57126, Indonesia.
[2]Department of Chemistry, Faculty of Mathematics and Natural Science, Universitas Sebelas Maret,
Surakarta 57126, Indonesia.

*Corresponding author email: candra_pr@staff.uns.ac.id

Received June 12, 2021; **Accepted** January 24, 2023; **Available online** March 20, 2023

ABSTRACT. The composite of Graphite/$PbTiO_3$ has been synthesized for photocatalyst and photo-electrocatalyst of Methyl Orange (MO) and Methyl Violet (MV) degradation using a visible light source. The aims of the research were to study the influence of pH of the solution, iradiation time and kinetics study of MO and MV photodegradation, voltage of photoelectrodegradation of MO and MV. Composite of Graphite/$PbTiO_3$ was synthesized by the sol-gel process with Titanium Tetraisopropoxide (TTIP) solution and $Pb(NO_3)_2$ powder as the precursors. Graphite/$PbTiO_3$ composite was characterized using X-ray difractometer and FTIR spectrometer. The diffractogram of Graphite/$PbTiO_3$ composite showed peaks at $2\theta = 26.507°$ as a characteristic diffraction of Graphite, and at $2\theta = 31.838°$ and 39.294° as those of $PbTiO_3$. FTIR spectrum of Graphite/$PbTiO_3$ composite exhibits vibration peaks of TiO_2 at 609.5 – 420.5 cm^{-1} and those of Pb-O at 1337.66 cm^{-1} until 1395.56 cm^{-1}. The photodegradation results showed that Graphite/$PbTiO_3$ composite can degrade MO and MV optimally at a pH = 3. The photodegradation levels of MO and MV were 90.33% and 88.26% for 30 min of visible light radiation, respectively. The photodegradation of MO and MV were following the first-order reaction with a reaction rate constant of 0.4445 min^{-1} and 0.4244 min^{-1}, respectively. Meanwhile, the photoelectrodegradation of MO was 96.50% at 10 volts and at pH 11, while the photoelectrodegradation of MV was 95.14% at 10 volts and at pH 7. When compared previous research, this result also shows excellent degradation MO and MV using Graphite/$PbTiO_3$ under visible light irradiation. So that the use of visible lights provides an advantage over the use of UV light.

Keywords: Graphite/$PbTiO_3$, Methyl Orange (MO), Methyl Violet (MV), Photodegradation, photoelectrodegradation, visible light

INTRODUCTION

Currently, the textile industry is one of the most developed industries in Indonesia, especially in Java Island. Routoula and Patwardhan (2020) explained that textile industry is known to be one source of water pollution. Saputra et al. (2020) state that negative impacts of textile production are primarily derived from the dyeing process resulting in dye wastewater. The waste is extremely harmful to the environment, especially to the river ecosystem in Indonesia. Rethinasabapathy et al. (2018) and Hariani et al. (2018) said that textile dyes are stable, difficult to degrade, toxic, mutagenic, and carcinogenic. Two examples of dyes usually used in the textile industry are Methyl Orange (MO) and Methyl Violet (MV).

Photocatalytic have been used in many applications such as energy production (Asiri et al., 2021), antibacterial agent (Rokicka-Konieczna et al, 2020), degradation for textile and pharmaceutical wastewater (Asiri et al, 2022; Chakraborty et al, 2017). TiO_2 is a good photocatalyst under UV irradiation but it has low efficiency under visible light irradiation (Vis) due to its large band gap (Cardona, 2022; Deng et al., 2019; Ghrib et al., 2021; Purnawan et al., 2016). TiO_2 has been modified using some additive to increase the photodegradation efficiency such as carbon/ semiconductor, metal oxide (Awfa et al., 2018), $TiO_2/ZnCr_2O_4$ (Salehi et al., 2019), TiO_2/wood charcoal (Luo et al., 2015), TiO_2/carbon nitride (Crake et al., 2019). Purnawan et al. (2016) and Purnawan et al. (2018) showed that Graphite/$PbTiO_3$ able to degrade textile waste water under UV irradiation and it can improve under electric current. Bhatti et al. (2016) concluded that $PbTiO_3$ is a ferroelectric material with the highest spontaneous polarization P_s among all the ferroelectric perovskites. Chaudhari and Bichile (2013) said that $PbTiO_3$ gives evidence of the ferroelectric in ceramics. And it will improve electron transfer so that can improve electrodegradation. Purnawan et al. (2016) and Purnawan et al. (2018) state that Graphite/$PbTiO_3$

semiconductor has been known as a photocatalyst material that has good chemical stability and has excellent photodegradation and photoelectrodegradation of MO and MV under UV irradiation. The results showed that the optimal composition of Graphite/$PbTiO_3$ was 1:1 at 10 volts for 30 min, pH 11 for MO degradation, and at pH 7 for MV degradation.

However UV light have a more dangerous impact on health and consume much energy so that it will increase the operational cost of Graphite/$PbTiO_3$ photocatalytic systems. To date, there has been no recent research on photodegradation and photoelectrodegradation of MO and MV using Graphite/$PbTiO_3$ under visible light irradiation. Therefore, this study will examine the photodegradation and photoelectrodegradation of MO and MV using visible light irradiation, and compare it with previous research. The photocatalytic and activity photoelectrocatalytic of $PbTiO_3$ will be influenced by several factors, such as pH solution, light source, voltage or current, and time irradiation (Lee et al., 2014; Mamaghani et al., 2019; Purnawan et al., 2018; Yang et al., 2022).

EXPERIMENTAL SECTION

Materials and General Methods

The research has used materials including: TTIP (titanium tetraisopropoxide) (Aldrich), $Pb(NO_3)_2$ (Merck), glacial acetic acid (Merck), graphite, silica adhesive (Autosil Black Gasket RTV Silicone), nitric acid (Merck), potassium chloride (Merck), chloric acid (Merck), sodium hydroxide (Merck), Methyl Orange (MO) and Methyl Violet (MV).

The composite was characterized using X-ray Diffraction (XRD, using Cu Kα), Fourier Transform Infra-red (FTIR, model Shimadzu Prestige 21, prepared in KBr pellet, scanned in range between 400-4000 cm^{-1}, with resolution of 4 cm^{-1}). Concentration of dyes solution, before and after treatments was measured using UV-Vis spectrophotometer (Model Itachi). Photocatalytic and photoelectrocatalytic degradation was performed using visible lamp Osram ultra vitalux (300W 230V AC).

Preparation of Graphite

The graphite rod was powdered and then emerged into a 0.1 M HNO_3 solution for 24 h. The mixture solution was filtered and washed with distilled water until neutral. Then, graphite powder was filtered and dried at room temperature. Graphite powder was sieved on 100 mesh size.

Synthesis of TiO_2

A 10 mL TTIP solution was hydrolyzed with 100 mL glacial acetic acid in a water bath (14 °C), stirred, and heated at 90 °C. The gel obtained was cooled at room temperature and oven at 150 °C for about 24 h. The white TiO_2 powder obtained was then calcined at 400 °C for 2 h to obtain TiO_2 anatase crystal.

Synthesis of $PbTiO_3$

Synthesis of $PbTiO_3$ was carried out by hydrolyzing the TTIP solution into glacial acetic acid (14 °C) in a ratio of 1:10 (v/v) and stirring it for 30 min. The mixture was heated at 90 °C to produce a white gel. Then, $Pb(NO_3)_2$ powder was added into the mixture and stirred for 5 – 10 min until the formation of sol. Finally, Graphite powder was added into the sol then heated at 150 °C for about 24 h, and calcined at 400 °C for 2 h.

Preparation of Graphite/$PbTiO_3$ Composite Electrode

Graphite/$PbTiO_3$ composite was mixed with silica adhesive with a ratio of 4:1 (w/w). The mixture is molded in an electrode mold with a pressure of 1000 psi to obtain a cylindrical electrode rod with a length of 2.5 cm and a diameter of 0.7 cm. Then, the electrode rod was heated at 120 °C for 6 h.

Photodegradation of MO and MV Using Visible Light

A 0.3 g of Graphite/$PbTiO_3$ powder was added into 30 mL solution of MO and MV 5 ppm with pH variation of 3, 5, 7, 9, and 11 and radiated for 5, 10, 15, 20, 25, and 30 min. The solution was stirred under visible light radiation of 300 watts in a reactor. The absorbance of MO and MV solution had been measured after 30 min, and before irradiation as control.

Photoelectrodegradation of MO and MV Using Visible Light

A 0.5 mg of MO and MV was dissolved into 100 mL KCl 0.1 M. Photoelectrodegradation process was conducted in a reactor with Graphite as cathode and Graphite/$PbTiO_3$ composite as an anode. The electrodes were immersed into 20 mL of MO and MV 5 ppm with a voltage variation of 2.5, 5.0, 7.5, 10, 12.5 Volt under visible light radiation for 30 min and then proceeded with a variation of pH = 3, 5, 7, 9 and 11 using optimum voltage.

RESULTS AND DISCUSSION

Characterization of TiO_2

The purpose of XRD characterization is to know the diffraction pattern of TiO_2 that has been synthesized. The diffraction pattern of synthesized TiO_2 is shown in **Figure 1**. The diffraction pattern of TiO_2 in **Figure 1** showed the diffractogram indicates that synthesized TiO_2 has anatase crystal phase with dominant peaks at 2θ of 25.320°; 37.860° and 48.060° (appropriate with JCPDS No. 78-2486).

Characterization of $PbTiO_3$

The characterization of $PbTiO_3$ powder at a calcination temperature of 400 °C results in the diffractogram pattern shown in **Figure 2**.

There are peaks 2θ at 31.480°; 32.461° and 39.217° that are characteristic peaks of $PbTiO_3$ and are appropriate with JCPDS No. 74-2495. Several peaks 2θ of PbO still appear at 28.361°; 35.289° and 41.840° that are appropriate with JCPDS standard No. 85-0711 and no TiO_2 peaks are found.

It shows that the addition of $Pb(NO_3)_2$ influences the formation of a new compound ($PbTiO_3$) which has different properties from TiO_2 and PbO.

Characterization of Graphite/$PbTiO_3$ Composite

The diffractogram of Graphite/$PbTiO_3$ shows a peak at $2\theta = 26.507°$ that is a characteristic peak of Graphite and peaks at $2\theta = 31.838°$; $39.294°$; $46.315°$ and $54.140°$ that are characteristic peaks of $PbTiO_3$ (**Figure 3**). Meanwhile, FTIR characterization of Graphite/$PbTiO_3$ composite is shown in **Figure 4.** FTIR analysis shows the functional group of $PbTiO_3$ and Graphite/$PbTiO_3$ composite.

There are differences in absorption peaks of TiO_2, $PbTiO_3$, Graphite, and Graphite/$PbTiO_3$ composite. Peaks at 1337.66 cm^{-1} to 1395.56 cm^{-1} regions are characteristic vibration of Pb-O and this is just owned by a compound containing Pb-O as like $PbTiO_3$ and Graphite/$PbTiO_3$ composite, whereas absorption in this region is not found in the FTIR spectra of Graphite and TiO_2.

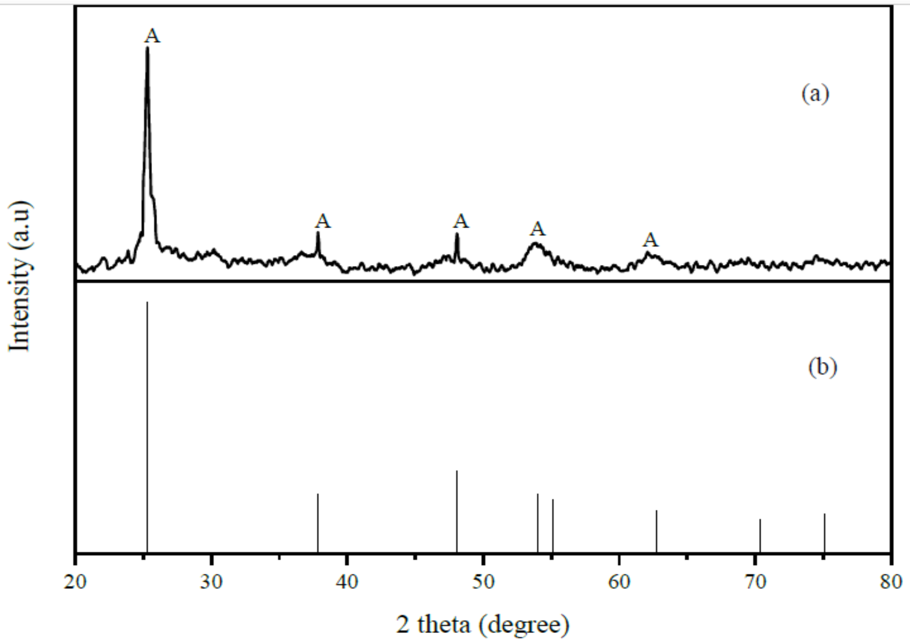

Figure 1. Difractogram of (**a**) synthesized TiO_2 and (**b**) standard of anatase TiO_2 (JCPDS No. 78-2486)

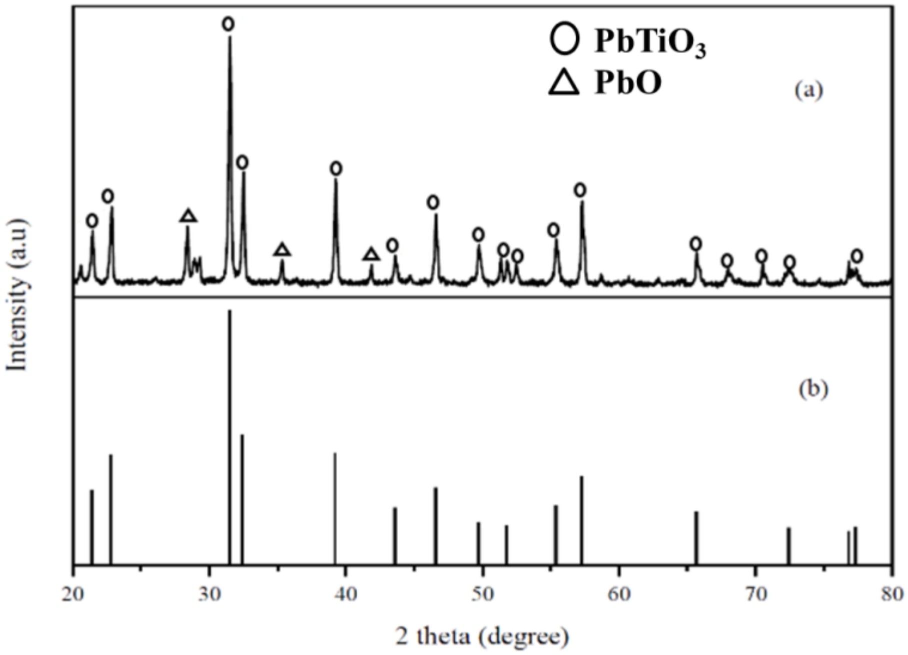

Figure 2. Diffractogram of (**a**) $PbTiO_3$ and (**b**) $PbTiO_3$ standard (JCPDS No. 74-2495)

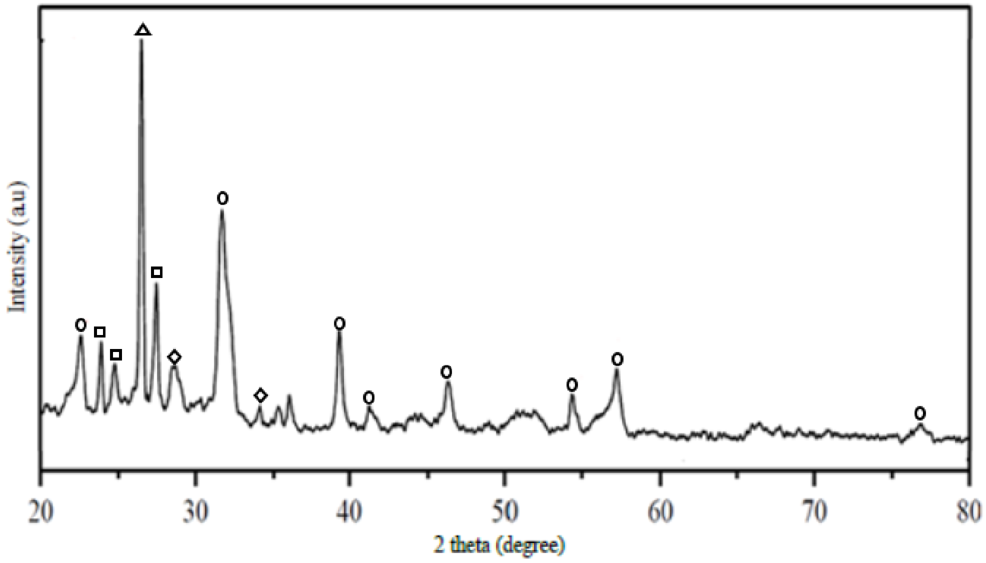

Figure 3. Diffractogram of Graphite/$PbTiO_3$ (1:1) composite (○=$PbTiO_3$, Δ=Graphite, □=Pb_2O_3, ◇=PbO).

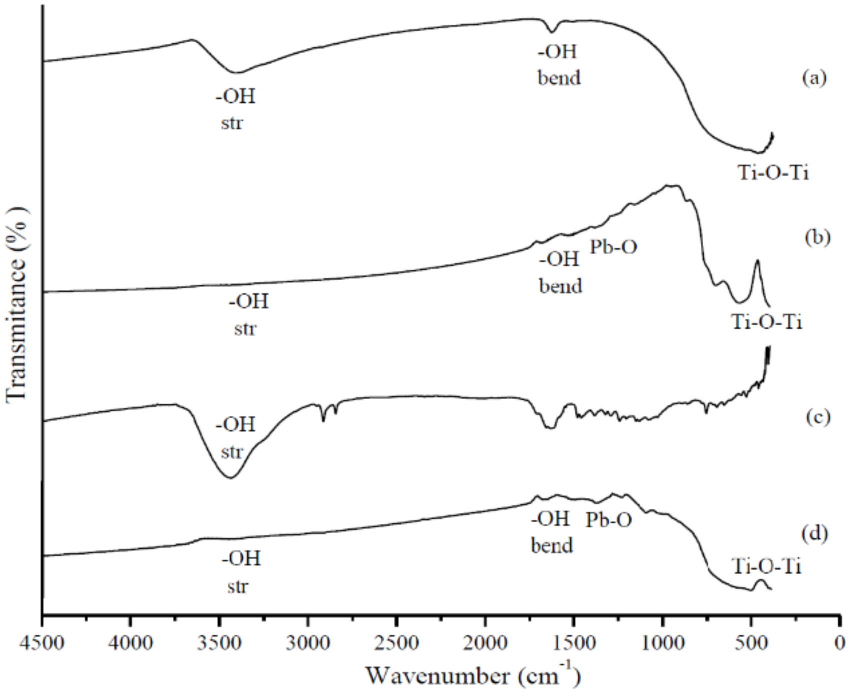

Figure 4. FTIR spectra of (**a**) TiO_2, (**b**) $PbTiO_3$, (**c**) Graphite and (**d**) Graphite/$PbTiO_3$ (1:1) composite

The Influence of pH Solution Variation on Photodegradation of MO and MV

The pH variations of the MO and MV dyes solutions used were 3; 5; 7; 9 and 11. The photodegradation results of MO and MV dyes for each pH were shown in **Figure 5**. The pH of the solution will affect the formation of the surface charge of the composite and the substrate, so it will affect the interaction between the composite and the substrate (Setyaningtyas et al., 2022).

Figure 5 shows the percentage of optimum photodegradation that occurs in the starting solution of MO at a pH of 3 is 90.33%. This result is caused by the effect of low pH value. At low pH value MO is protonated to positive charge so the affinity on hydroxyl radical (•OH) reaction and superoxide (O_2^-) anion radical are higher. The addition of HCl to obtain acid pH influences the percentage of MO degradation. Anion Cl^- in the solution can be oxidized to Cl_2 or ClO_3^-, which is a strong oxidizing agent where along with hydroxyl radical can degrade dyes so, the degradation percentage of methyl orange higher at acid pH. Reduction-oxidation reaction under photocatalys irradiation following equation 1-3. The reaction can take place with the initiation of light radiation against the photocatalyst.

$$PbTiO_3 + hu \rightarrow h^+_{vb} + e^-_{cb} \quad (1)$$
$$2H_2O + 2e^- \rightarrow H_2 + 2OH^- \; E^0_{red} = -0{,}83 \text{ volt} \quad (2)$$
$$2Cl^- + 2h^+ \rightarrow Cl_2 \; E^0_{red} = +1{,}36 \text{ volt} \quad (3)$$

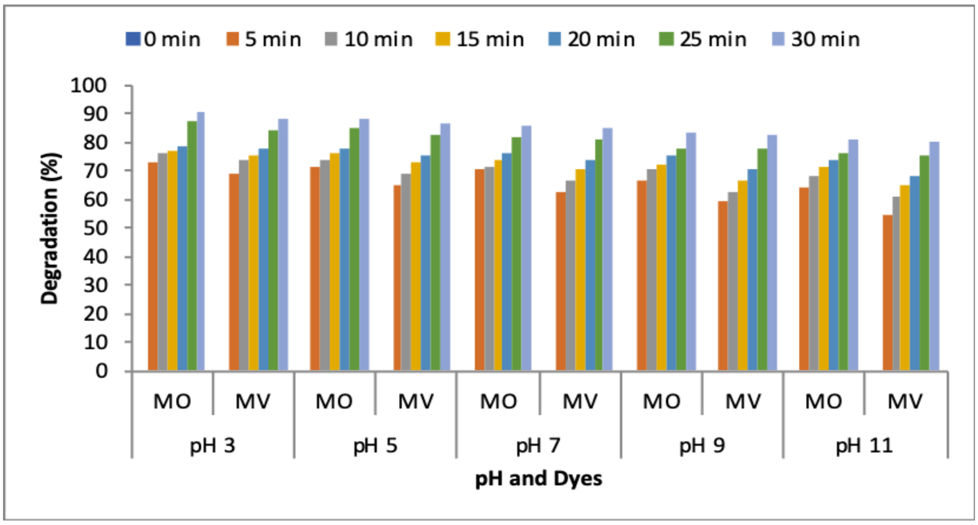

Figure 5. Photodegradation activity (%) in solution pH variation of MO and MV

Then, MV dye has an optimum degradation percentage of 88.26% in a starting solution with a pH of 3. MV dye at neutral condition will be split in their cation and anion. In acid pH conditions (3 and 5), a cation that contains a chromophore group in the compound of MV will interact with H^+ ion from acid. The interacting H^+ ion impacts nitrogen (N) atom that binds hydrogen (H) atom and methyl group (CH_3) will release CH_3 group and bind with H atom from an acid. The nitrogen atom that binds 2 atoms causes the positive partial charge (δ^+) in the N atom higher than without binds methyl group and H atom. This affects the increasing affinity of hydroxyl (OH^-) radical reaction and superoxide (O_2^-) anion radical. Figure 5 has shown the longer the time the greater the degradation.

The Influence of Time Contact on Degradation and Kinetics of MO and MV Degradation

Photodegradation results of MO and MV dyes solution for each contact time are shown in **Figure 6** and **Figure 7**. It shows that the longer the time, the greater the degradation of MO and MV. The highest degradation percentage had been achieved by Graphite/$PbTiO_3$ with a percentage of 90.05% for MO and 88.00% for MV for 30 minutes of radiation.

Kinetics study for degradation rate has been conducted by calculating its reaction rate constant. Photodegradation kinetics of MO and MV for graphite/$PbTiO_3$ composite prefer follows first-order reaction kinetics with the reaction rate constant (*k*) of respectively 0.4445 min^{-1} and 0.4244 min^{-1}. The curve of kinetic of MO and MV are shown in **Figure 8** and **Figure 9**. The reaction rate constant of MO degradation was higher than the reaction rate constant of MV degradation. That means that MO degradation was faster than MV degradation. It is because of the molecule structure of MV more stable than MO. The presence of Sulfonate groups (S=O) and a nitrile ion group (HN^+=N-) in MO causes it to be more reactive so that it readily reacts and is easily degraded. Besides, the molecular weight of MO is smaller than MV so that it is degraded more quickly.

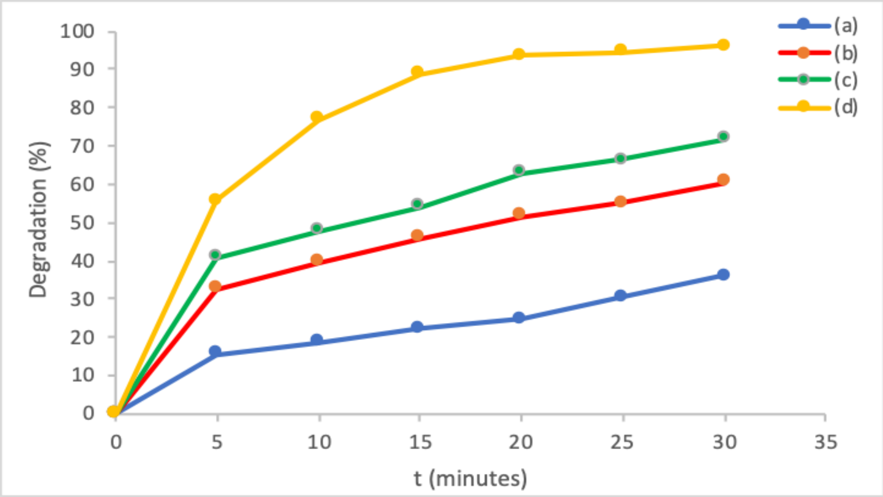

Figure 6. Methyl orange degradation (%) with radiation times variation using (**a**) Graphite, (**b**) TiO_2, (**c**) $PbTiO_3$ and (**d**) Graphite/$PbTiO_3$ composite

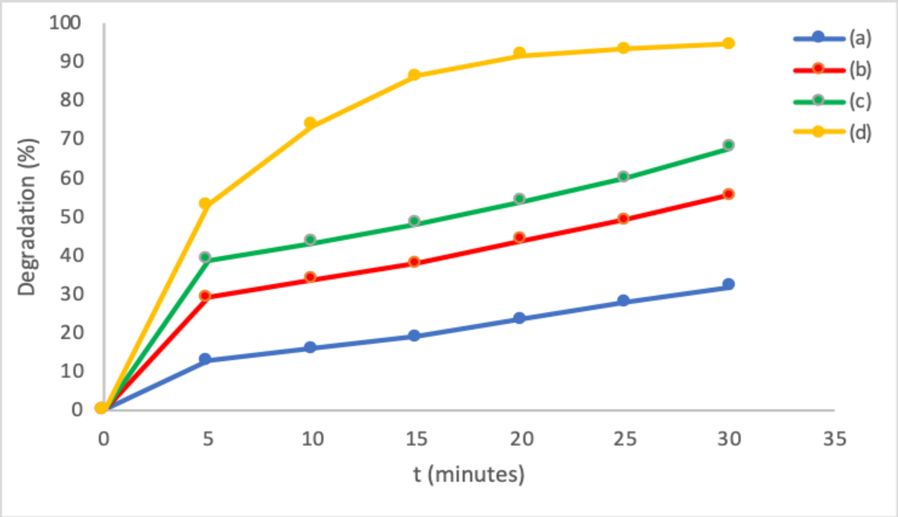

Figure 7. Methyl violet degradation (%) with radiation times variation using (a) Graphite, (b) TiO_2, (c) $PbTiO_3$ and (d) Graphite/$PbTiO_3$ composite

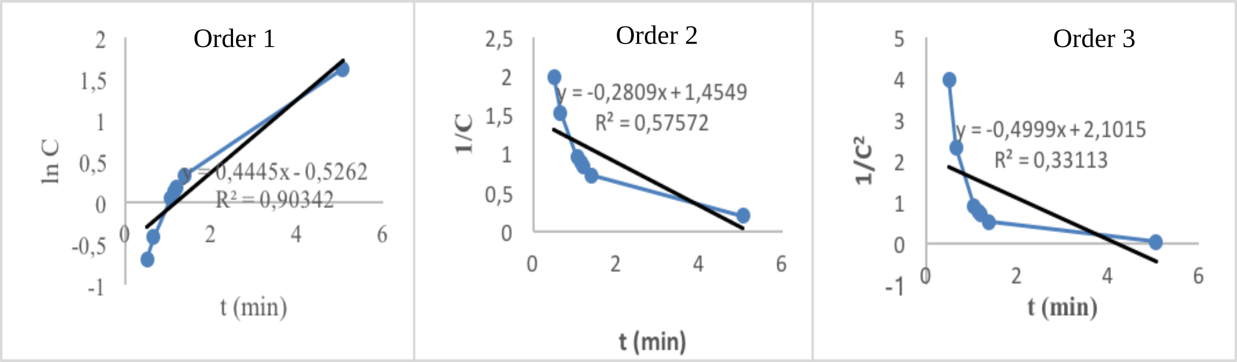

Figure 8. Kinetics of MO photodegradation using visible light

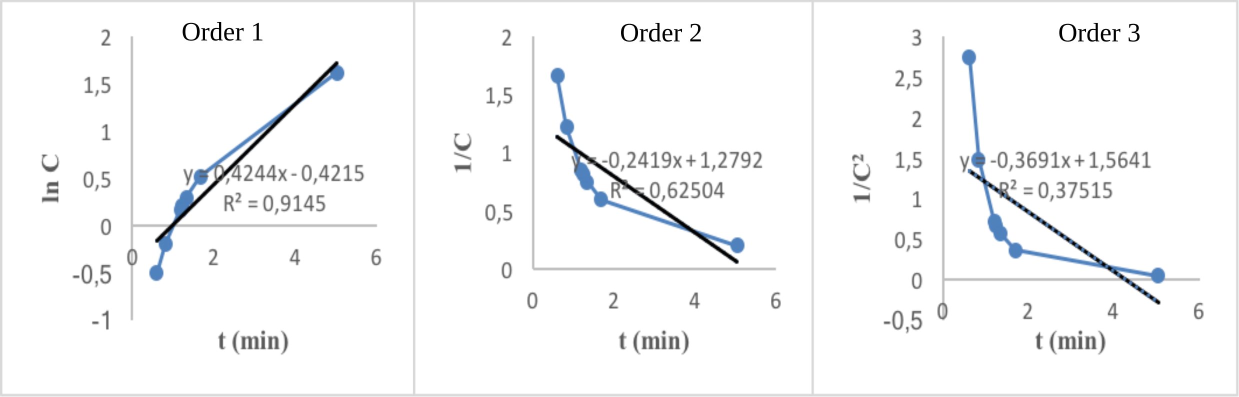

Figure 9. Kinetics of MV photodegradation using visible light

The Influence of Voltage on Photoelectrodegradation of MO and MV

The voltage variations of the MO and MV dyes solutions used were 2.5; 5.0; 7.5; 10.0 and 12.5 volts. He et al. (2003) concluded that the outside potential in the electrolysis system is not only can separating electrons on conductive band from oxidation process, but also reducing the electron-hole recombination and separating the oxidation and reduction sides. Linsebigler et al. (1995) and Purnawan et al. (2018) said that TiO_2 and $PbTiO_3$ are also electrochemically oxidized forming electron (e^{-}_{cb}) and hole (h^{+}_{vb}). The hole (h^{+}_{vb}) could initiated the oxidation reaction and in other side the e^{-}_{cb} initiated reduction reaction in the semiconductor surfaces. The occurring reduction-oxidation reaction mechanism is that h^{+}_{vb} oxidized water or hydroxyl group of MO and MV adsorbed in the material surfaces to form a hydroxyl radical ($OH^{\cdot}$). However, in the same times, e^{-}_{cb} reduced the adsorbed oxygen to form superoxide and hydroperoxide radical anions. Degradation of MO and MVt performed because of the electrocatalytic and photocatalytic processes. By placing graphite electrode in catode and the graphite/$PbTiO_3$ composite in anode, the possible reaction probably occurred at each electrodes following equation 4-14.

Reaction in Cathode

$2H_2O + 2e^- \rightarrow H_2 + 2OH^-$ (4)

Reaction in Anode

Electrocatalytic process

$2Cl^- \rightarrow Cl_2 + 2e^-$ (5)

$2H_2O \rightarrow 4H^+ + O_2 + 4e^-$ (6)

Photocatalytic Process

$PbTiO_3 + hu \rightarrow h^+_{vb} + e^-_{cb}$ (7)

$e^-_{cb} + O_2 \rightarrow O_2^\cdot$ (8)

$2O_2^\cdot + 2H_2O \rightarrow H_2O_2 + 2OH^- + O_2$ (9)

$H_2O_2 + e^-_{cb} \rightarrow OH^\cdot + OH^-$ (10)

$h^+_{vb} + OH^- \rightarrow OH^\cdot$ (11)

$h^+_{vb} + H_2O \rightarrow H^+ + OH^\cdot$ (12)

$OH^\cdot$ + MO or MV → simple compound (13)

$O_2^\cdot$ + MO or MV → simple compound (14)

The photoelectrodegradation results of MO and MV dyes for each voltage are shown in Figure 10. **Figure 10** shows the higher the voltage the greater the degradation of MO and MV until reaching an optimum point (10.0 volt). The higher voltage results in a faster electric current from cathode to anode. Consequently, the electron movement rate from the valence band to the conductance band is higher. Therefore, the photoelectrocatalytic activity of composite increases. At 10.0 volts, degradation of MO was 92.11% and degradation of MV was 90.28%, which decreased to 77.68% for MO degradation and 72.22% for MV degradation at 12.5 volts. This occurs because of the higher electric current on the electrode and faster collision between electron that causes the gasses from photoelectrodegradation process covers the anode surface so visible light interaction and oxidation at the anode is disturbed and photocatalytic activity decreased.

The Influence of pH on Photoelectrodegradation of MO and MV

The pH variations of the MO and MV dyes solutions used were 3; 5; 7; 9; and 11 with a voltage of 10.0 volt. The photoelectrodegradation results of MO and MV dyes for each pH solution are shown in **Figure 11**.

Figure 11 shows the photoelectrodegradation of methyl orange and methyl violet that is optimum under pH = 11 and pH = 7, respectively. In acid pH (3 and 5), methyl orange works as a cation (positive charge in N atom). The cationic methyl orange approaches on the cathode (graphite electrode) that has a negative charge so methyl orange concentration at acid pH decreases. However, the positive charge of methyl orange keeps away from TiO_2 in graphite/$PbTiO_3$ composite so catalytic activity is lower than basic pH with a degradation percentage of 93.35% at 3 pH and 94.39% at 5 pH. In the higher pH condition (pH of 7), methyl orange is formed zwitterion (**Figure 12**). The capability of approaching electrode is weaker than cation formed because there is no movement of charge to anode or cathode so catalytic activity is lower than acid pH with degradation percentage of 89.00%. In the basic pH (9 and 11), methyl orange is formed anion. Because of that, methyl orange will close anode (graphite/$PbTiO_3$ composite electrode) that has a positive charge so the concentration of methyl orange decreases. In the anode, hydroxyl radical is formed and will react to dye so that concentration of methyl orange decreasing higher with degradation percentage of 95.62% (pH of 9) and 96.50% (pH of 11).

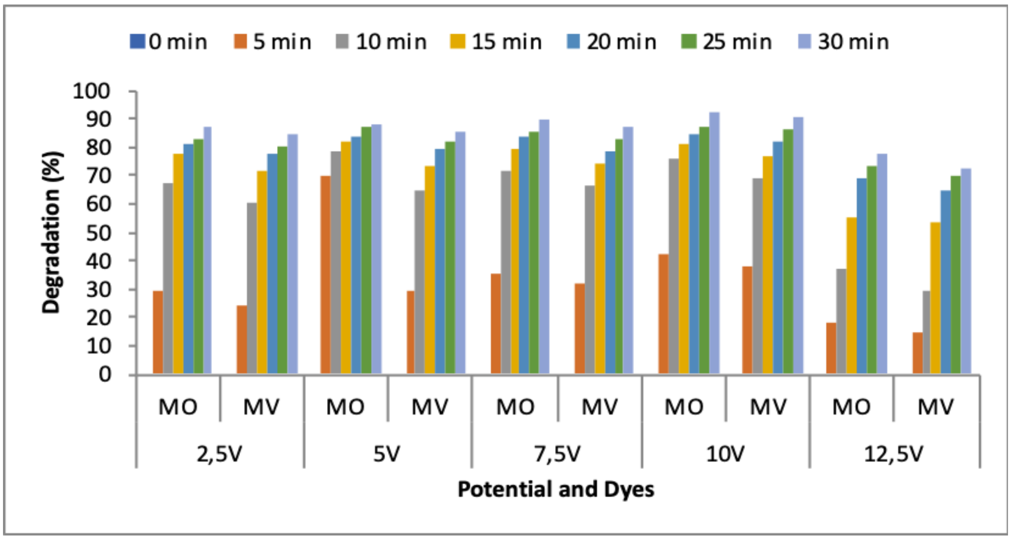

Figure 10. Photoelectrodegradation (%) of MO and MV at voltage variation

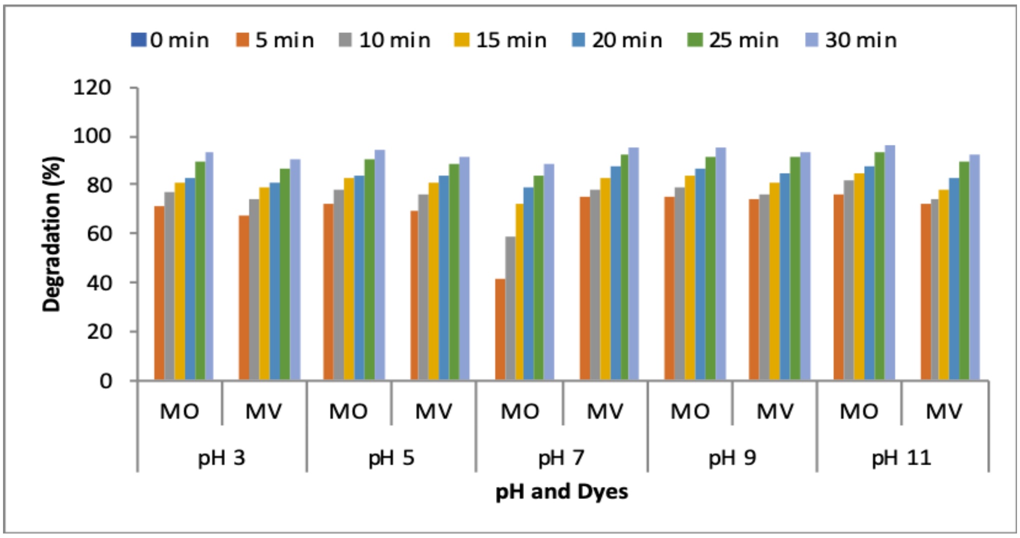

Figure 11. Photoelectrodegradation (%) of MO and MV at pH solution variation

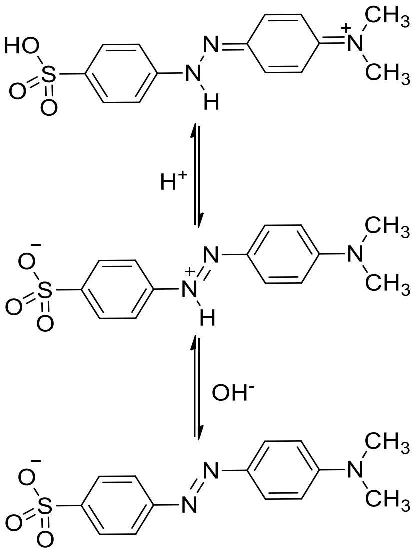

Figure 12. Structure of methyl orange under acid, neutral and basic condition

Methyl violet dye splits into cation and anion under neutral condition, as shown in **Figure 13**. In the acid condition (3 and 5), the cation containing chromophore group will interact with H^+ ion from acid. Saeed et al. (2010) explained that interaction of H^+ ion causes N atom that binds H and CH_3 will release CH_3 group and then binds with H atom from an acid.

When N atom binds 2 H atoms, it will have a positive partial charge (δ^+) that is stronger than it just binds with 1 H atom. The chromophore group will stay away from the anode (positive pole) because of the repulsion force between its charges so photoelectrodegradation process will be inhibited. Therefore, if N atom bind 2 atoms of H so steric factor will be smaller because the binding angle is more symmetric. In this condition, Cl (δ^-) has a lower negative charge than the neutral condition because the bond length between N (δ^+) and Cl (δ^-) is lower. It is different from a neutral condition where N atom binds 1 methyl group and 1 H atom, so CH_3 pushes the electron to Cl (δ^-) atom. Therefore, then Cl has many electrons and the negative partial charge is higher. Because of that, under neutral conditions, Cl (δ^-) makes the movement of cationic dye to anode easier. Thus, under neutral conditions (pH of 7), the concentration degradation of dyes will be better than under acid conditions. The possible structure of methyl violet under acidic condition was given in **Figure 14**. **Figure 15** shows the structure of methyl violet under basic condition. According on reseach by Purnawan, et al. (2018), In the basic pH condition (9 and 11), the resonance form of cation containing chromophore group in methyl violet compound will interact with OH^- ion from basic. The oxygen atom in OH^- group has electronegative properties and free-electron pair that can place the electron vacancy in an anode. Therefore, under basic condition, the degradation capability on methyl violet is higher than under acid condition.

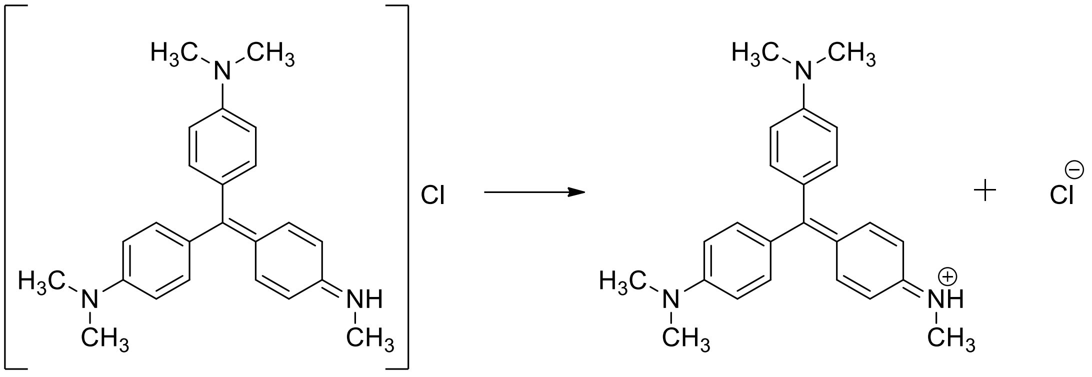

Figure 13. Ionization of methyl violet dye

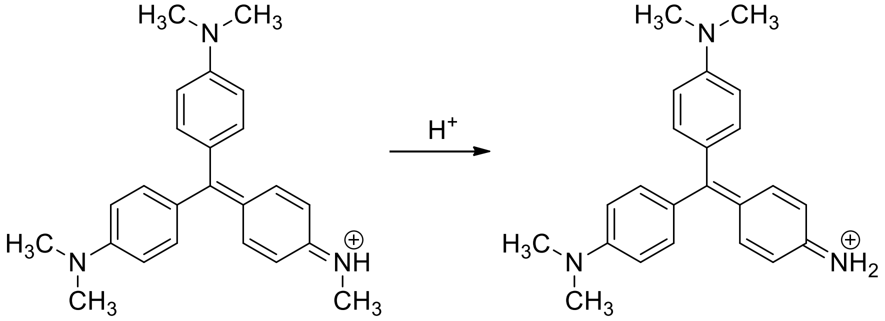

Figure 14. Structure of methyl violet at the acid condition

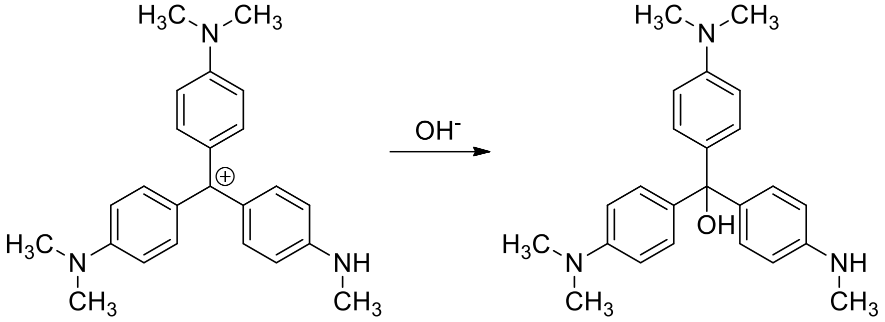

Figure 15. Structure of methyl violet under basic condition

CONCLUSION

The optimum condition of pH in photodegradation process was pH = 3 with a degradation percentage of 90.33% for methyl orange (MO) and 88.26% for methyl violet (MV). The optimum condition of degradation percentage of MO and MV is achieved in 30 min of radiation time. The optimum voltage to degrade MO and MV was 10 volt with a degradation percentage of 97.60% for MO and 95.50% for MV. The Optimum condition of pH in photoelectrodegradation process was pH = 11 for MO (96.50%) and pH = 7 for MV (95.14%) at 30 minutes. When compared UV irradiation, this result also shows excellent degradation MO and MV using Graphite/$PbTiO_3$ under visible light irradiation. So that the use of visible lights provides an advantage over the use of UV light.

REFERENCES

Asiri, A. M., Nawaz, T., Tahir, M, B., Fatima, N., Khan, S, B., Alamry, K, A., Alfifi, S, Y., Marwani, H, M., Al-Otaibi, M, M., and Chakraborty, S., 2021. Fabrication of WO_3 based nannocomposites for the excellent photocatalytic energy production under visible light irradiation. *International Journal of Hydrogen Energy*, *46*, 39058 – 39066.

Asiri, A. M., Pugliese, V., Petrosino, F., Khan, S. B., Alamry, F. A., Alfifi, S. Y., Marwani, H. M., Alotaibi, M. M., Mukherjee, D., and Chakraborty, S., 2022. Photocatalytic degradation of textile dye on blended cellulose acetate membranes. *Polymers*, 14, 636.

Awfa, D., Ateia, M., Fujii, M., Johnson, M. S., Yoshimura, C. 2018. Photodegradation of pharmaceuticals and personal care products in water treatment using carbonaceous-TiO_2 composites: a critical review of recent literature. *Water Research, 142*, 26–45.

Bhatti H.S., Hussain S.T., Khan, F.A., Hussain, S., 2016. Synthesis and induced multiferroicity of perovskite pbtio$_3$; A Review. *Applied Surface Science, 36*, 291-306.

Cardona, Y., Wegrzyn, A., Miskowiec, P., Korili, S. A., Gil, A. 2022. Catalytic Photodegradation of organic compounds using TiO_2/pillared clays synthesized using a nonconventional aluminum source. *Chemical Engineering Journal,* 446, 136908.

Chakraborty, S., Loutatidou, S., Palmisano, G., Kujawa, J., Mavukkandy, M, O., Al-Gharabli, S., Curcio, E and Arafat, H, A., 2017. Photocatalytic hollow fibeer membranes for the degradation of pharmaceutical compounds in wastewater. *Journal of Environmental Chemical Engineering, 5* (2017), 5014 – 5024.

Chaudhari, V.A., and Bichile, G.K., 2013. Synthesis, structural, and electrical properties of pure $PbTiO_3$ ferroelectric ceramics. *Smart Materials Research*, *2013*, 1-9.

Crake, A., Christoforidis, K. C., Godin, R., Moss, B., Kafizas, A., Zafeiratos, S., Durrant, J. R., Petit, C. 2019. Titanium dioxide/carbon nitride nanosheet nanocomposites for gas phase CO_2 photoreduction under UV-visible irradiation. *Applied Catalysis B*, *242*, 369–378.

Deng, H., Wang, Y., Zhang, X., Kou, X., Chen, B., Zhu, C. 2019. Photodegradation under natural indoor weak linght assisted adsorption of X-3B on TiO_2/Al_2O_3 nanocomposite. *Chemical Engineering Journal,* 372.

Ghrib, T., AL-Saleem, N.K., AL-Naghmaish, A., Elshekhipy, A. A., Brini, S., Briki, K., Elsayed, K. A. 2021. Annealing effect on the microstructural, optical, electrical, and thermal properties of Cu_2O/TiO_2/Cu_2O/TiO_2/Si heterojunction prepared by solgel technique. *Superlattices Microstruct*, 107119.

Hariani, P.L., Faizal, M., Ridwan, Marsi, Setiabudidaya, D., 2018. Removal of Procion Red MX-5B from songket's industrial wastewater in South Sumatra Indonesia using activated carbon-Fe_3O_4 composite. *Sustainable Environment Research* 28, 158–164.

He, C., Xiong, Y., Zha, C., Wang, X., Zhu, X., 2003. Approach to pulse photoelectrocatalytic process for the degradation of organic pollutants. *Journal of Chemistry Technology Biotechnology, 78*, 717–723.

Lee, D. S., Lee, S. Y., Rhee, K., Park, S. J. 2014. Effect of hydrothermal temperature on photocatalytic properties of TiO_2 nanotubes. *Current Applied Physics, 14*, 415–420.

Linsebigler, A. L., Lu, G., Yates, J. T. Jr., 1995. photocatalyst on TiO_2 surface: principles, mechanisms, and selected result. *Chemical Reviews, 95*, 735–758.

Luo,L., Yang, Y., Xiao, M., Bian, L., Yuan, B., Liu, Y., Jiang, F., Pan, X. 2015. A novel biotemplated synthesis of TiO_2/wood charcoal composites for synergistic removal of bisphenol A by adsorption and photocatalytic degradation. *Chemical Engineering Journal,* 262: 1275–1283.

Mamaghani, A.H., Haghighat, F., Lee, C.S. 2019 Systematic variation of preparation time, temperature, and pressure in hydrothermal synthesis of macro-/mesoporous TiO_2 for photocatalytic air treatment. *Journal of Photochemistry Photobiology A*, 2019, *378*, 156–170.

Purnawan, C., Wahyuningsih, S., Kusuma, P.P., 2016. Photocatalytic and photoelectrocatalytic degradation of methyl orange using graphite/$PbTiO_3$ composite. *Indonesian Journal of Chemistry, 16* (3), 347–352.

Purnawan, C., Wahyuningsih, S., Nawakusuma, V., 2018. Methyl violet degradation using photocatalytic and photoelectrocatalytic processes over graphite/$PbTiO_3$ composite. *Bulletin of Chemical Reaction Engineering & Catalysis, 13*(1), 127–135

Rethinasabapathy, M., Kang, S.M., Lee, I., Lee, G.W., Hwang, S.K., Roh, C., Huh, Y.S., 2018. Layer-structured POSS-modified Fe-Aminoclay/carboxymethyl cellulose composite as a superior adsorbent for the removal of radioactive cesium and cationic dyes. *Industrial & Engineering Chemistry Research,* 57, 13731–13741

Rokicka-Konieczna, P., Wanag, A., Sienkiewicz, A., Kusiak-Nejman, E., & Morawski, A. W., 2020. Antibacterial effect of TiO_2 nanoparticles modified with APTES. *Catalysis Communications, 134*, 105862.

Routoula, E., Patwardhan, S. V., 2020. Degradation of anthraquinone dyes from effluents: a review focusing on enzymatic dye degradation with industrial potential. *Environmental Science & Technology, 54*, 647–664

Saeed, R., Ashfaq, M., Fahimuddin, 2010. Spectrophotometric study on kinetics of solvatochromism of methyl violet in aqueous methanol. *Chinese Journal of Chemistry, 28*, 891–895.

Salehi, M., Eshaghi, A., Tajizadegan, H. 2019. Synthesis and characterization of TiO_2/ $ZnCr_2O_4$ core-shell structure and its photocatalytic and antibacterial activity. *Journal of Alloys and Compounds,* 778: 148–155.

Setyaningtyas, T., Kurniasih, M., Azizi, A.D.A.N., Riyani, K., Kartika, D., 2022. Synthesis of chitosan for removal of methyl orange and malachite green dyes. *AIP Conference Proceedings,* 2553, 020005 (2022); https://doi.org/10.1063/5.0103999

Saputra, O.A., Kurnia, Pujiasih, S., Rizki, V.N., Nurhayati, B., Pramono, E., Purnawan, C., 2020. Silylated-montmorillonite as co-adsorbent of chitosan composites for methylene blue dye removal in aqueous solution. *Communications in Science and Technology*, *5*, 45–52.

Yang, G., Li, Z., Peng, S., Yue, J., and Guo, Z. H.D., 2022. Synthesis of $PbTiO_3$ nanoplates by two-step hydrothermal method with ph-adjusting agent of ammonia solution. *Journal of Asian Ceramic Societies. 10* (2), 405-413